*Proceedings of the 2018 Winter Simulation Conference*
*M. Rabe, A.A. Juan, N. Mustafee, A. Skoogh, S. Jain, and B. Johansson, eds.*

# OPTIMISATION OF NAVAL GUN FIRING PATTERNS FOR ENGAGEMENT OF MANOEUVRING SURFACE TAGRGETS

Peter J. Young
Centre for Operational Research and Analysis
Defence Research and Development Canada
Canadian Forces Maritime Warfare Centre
Halifax, NS B3K 5X5, CANADA

## ABSTRACT

The problem of determining optimal naval gun firing patterns for engagement of manoeuvring surface targets using traditional simulation approaches is computationally intensive, particularly for large salvo sizes. A simplified modelling technique based on representing warhead effects using Gaussian function approximations calibrated from more detailed modelling is reported here. The simplified model permits the parameter space defining lay-down of rounds in a firing pattern to be searched so as to determine optimal patterns that maximise salvo probability of kill. The method employs Newton's method to formulate a system of equations defining local extrema, which are then solved using Gaussian elimination. These extrema are then searched to obtain the pattern that maximises salvo kill probability. This paper presents the underlying theory and gives initial results obtained using the model calibrated for an illustrative example from a more detailed model.

## 1 INTRODUCTION

A naval gun system can engage a manoeuvring surface target by firing a salvo of rounds at a predicted position of the target. Engagement success is compounded by possible target manoeuvres which occur during the fly out of the rounds to their aim points. Target manoeuvres can be countered by adopting a firing pattern where the rounds in a salvo are laid across a movement zone defined by possible target manoeuvres considered across the flight time of the rounds. A firing pattern is therefore defined as a set of aim points laid across a projected movement zone for the target. A problem of interest is to determine aim points for individual rounds in a salvo so as to maximise the salvo's kill probability against a manoeuvring target. These aim points can then be employed by a gun fire control system when engaging a target given its range, velocity and manoeuvre assumptions.

Friedman (2013) provides a general discussion of the employment of firing patterns by navies to combat manoeuvring targets. For analysis purposes, Monte Carlo simulations employing models for target tracking, projectile ballistics and warhead effects permit investigation of firing patterns given engagement situation assumptions. These models can be used to determine firing patterns for employment by naval gun systems. A restriction with this approach, however, is the extensive parameter space requiring study so as to determine optimal firing patterns, particularly as the problem size grows combinatorically with increase in salvo size.

Analytical techniques offer potential to complement Monte Carlo simulation by helping to rapidly explore a large parameter space and identify areas for more detailed study with simulations. As an example, Mirshak et al. (2010) used Monte Carlo simulations to determine of probability of kill per burst for ship defence against small boat attack. The specific problem of determining round placement within a firing pattern for defence against small boat attack has been considered by Young (2017), and it is this work that provides the problem context for the analysis presented here.

## 2 PROBLEM DESCRIPTION

The engagement problem can occur when a ship is defending itself from attack by one or more small manoeuvring boats. For a single target the defending ship fires a salvo of rounds from a single gun system at a projected target location. The aim point for an individual round aim can be obtained from a ballistics solution of the projectile intercepting the target taking into account projected target movement over the fly-out time of the projectile. Round effectiveness will therefore depend on the tracking accuracy, target velocity, range-to-target, projectile ballistics and warhead effects. The problem is further compounded by the target manoeuvring after the firing of the round. Salvo fire, with round detonation times staggered by the gun firing rate, permit increased engagement success – partly by the increased opportunities to kill the target, but also due to a lay down of fire across locations arising from possible target manoeuvres.

A general problem description is given in Young (2017), who also presented techniques to obtain salvo kill probability by integrating the aim point lethal zone for each round in the salvo across the target movement zone. As the rounds detonate sequentially, the target movement zone is updated for each consecutive round given the detonation points of the previous rounds. The target movement zone is also projected forward in time to the detonation time for the next round. Given the dependence of individual round kill probabilities on placement of earlier round aim points, the problem is computationally intensive to solve through simulation, solution time growing exponentially as the salvo size increases.

Figure 1(a), taken from Young (2017), shows the following key aspects of the problem, represented as probability distributions, for a 4-round salvo against a target approaching the firing ship:

- Target track distribution at the time the salvo commences to fire, shown in blue. This distribution results from target tracking errors and comprises target location, heading and velocity. The mean direction of travel for the target in Figure 1(a) is from right to left.
- Target movement zone, shown in green. This applies target manoeuvre assumptions over the target location distribution for the time period of the projectile fly-out following the firing of the gun. The movement zone will grow and translate to the left as each subsequent round in the salvo arrives and detonates. The zone shown in Figure 1(a) is for the last round of the 4-round salvo.
- Aim point lethal zone, shown in yellow/orange, laid over a portion of the target movement zone. The aim point lethal zone arises from an aggregation of the warhead lethal zone across a probability distribution for warhead detonation which results from projectile ballistic dispersion errors given an aim point. The warhead lethal zone for a given detonation point comprises target kill probabilities across locations relative to the detonation point. The kill probabilities are obtained from a warhead fragmentation model.
- Maximum Probability of Kill ($P_{K\_MAX}$) curves for each round in the salvo. Each curve stretches across the breath of the target movement zone at the time of the round's detonation. Each point on a $P_{K\_MAX}$ curve represents the optimal lead offset, ahead of the target track (the horizontal direction from right to left in Figure 1(a), for the aim point to maximise kill probability given the corresponding lateral offset [in the vertical direction of Figure 1(a)].

Young (2017) demonstrates how to construct the $P_{K\_MAX}$ curves numerically and use them to determine salvo $P_K$. The dependence of warhead $P_K$'s for each round on lateral distance across its corresponding $P_{K\_MAX}$ curve is shown in Figure 1(b). Salvo $P_K$ is obtained by, in sequence: placing each round at a position on its $P_{K\_MAX}$ curve, updating the target movement zone to reflect target survivability from the round, projecting the movement zone to the detonation time of the next round, and constructing the next round's $P_{K\_MAX}$ curve. The $P_{K\_MAX}$ curves for the second and subsequent rounds therefore depend on placement of earlier rounds. This makes the process computationally intensive for determination of an optimal placement of all rounds so as to maximise salvo $P_K$.

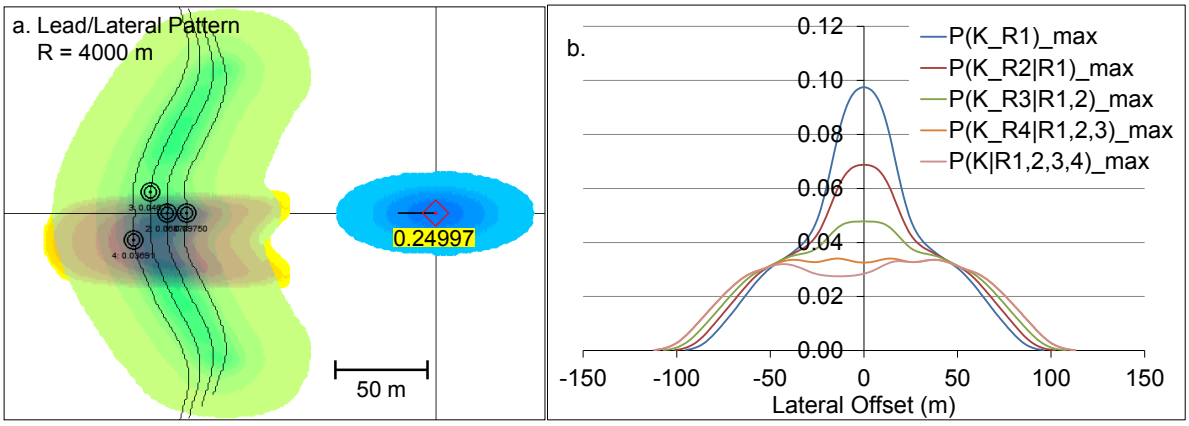


Figure 1: Four round results from Young (2017): (a) round laydown; (b) warhead $P_K$ dependence on lateral distance from $P_{K\_MAX}$ curves.

The firing pattern shown in Figure 1(a) was obtained using the following heuristic approach:

- The first and second rounds were placed at offsets corresponding to the peaks of their $P_{K\_MAX}$ curves so as to maximise their kill probabilities, i.e. 0 m lateral offset for rounds 1 and 2 with corresponding $P_K$'s of 0.09750 and 0.06878.
- A local search about the round 3 $P_{K\_MAX}$ curve peak was performed for placement of its aim point so as to maximise salvo $P_K$. For each round 3 position considered, the $P_{K\_MAX}$ curve for round 4 was reconstructed and used to position round 4 at its peak. This process yielded offsets of 9.6 m and -14 m with $P_K$'s of 0.04706 and 0.03660 for rounds 3 and 4. The resulting salvo $P_K$ was 0.24997.

This heuristic approach is not guaranteed to produce a global optimum. For larger salvo sizes a greater degree of local search would have to be employed to prevent excessive computer run times, but potentially reducing the "goodness" of the solution found. The remainder of this paper outlines an alternative method investigated to permit determination of firing patterns which maximise salvo $P_K$.

A simplified modelling technique is presented which adopts Gaussian function approximations for maximum probability of kill curves and warhead effects. The approach permits local extrema defining firing patterns that maximise salvo probability of kill to be found. Newton's method is used to formulate a system of equations defining local extrema, which are then solved using Gaussian elimination. This approach, a computer implementation and its application for an illustrative example are described below. The application involves calibration of the simplified model using outputs taken from Young (2017), which is also used to evaluate the results from the simplified model.

## 3 CONCEPTUAL BASIS FOR APPROXIMATING WARHEAD EFFECTS

An inspection of the plots for warhead $P_K$ dependence on $P_{K\_MAX}$ lateral offset given in Figure 1(b) shows that the effects for each round given its lateral offset are to reduce the $P_{K\_MAX}$ plot for the next round. This is better illustrated by transforming warhead effects for all rounds to the $P_{K\_MAX}$ curve for the last round, as shown in Figure 2. The ordinate for the plots in Figure 2 is a transformed $P_K$. Corresponding round $P_K$'s can be obtained by reversing the transformation back to the round's $P_{K\_MAX}$ curve. For example, a $P_K$ of 0.06685 for round 1 at the peak of its transformed $P_{K\_MAX}$ curve in Figure 2 corresponds to an actual $P_K$ of 0.09750 in Figure 1(b).

The warhead effects for each round are explicitly shown in Figure 2 by taking the difference between $P_{K\_MAX}$ plots for successive rounds. The difference between the P(K_R1)_max and P(K_R2|R1)_max plots is the d1 plot, this reflecting the round 1 warhead effects on killing the target. Plots d2, d3, and d4 are similarly defined.

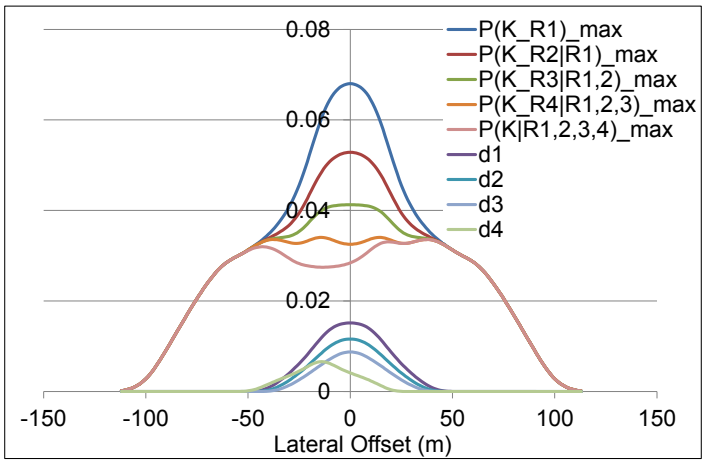


Figure 2: Warhead effects for rounds 1 to 4 mapped to $P_{K\_MAX}$ curve for round 4.

Changes in the lateral offset placement of rounds on their $P_{K\_MAX}$ curves result in their warhead effects plots being translated to the left (for increasing offset) or right (for decreasing offset). Inspection has found the warhead effects plots retain their shape as they translate for changing offset. This property is investigated below as a mechanism for determining transformed $P_K$ plots and using this as a basis for finding optimal firing patterns. The approach is illustrated for the four round example by the following: calibration of the d1, d2 and d3 plots; direct placement of the d1 plot; update of the P(K_R2|R1)_max plot by subtracting the displaced d1 plot from P(K_R1)_max; repeat for rounds 3 and 4 to yield the salvo $P_K$.

The approach is formalized by adoption of the following notation:

- For a salvo of $n = 4$ rounds, find $x_1, x_2, x_3, x_4$ that maximises the salvo probability of kill.
- $p_1(x)$ is the 1st round $P_K$ as a function of the variable $x$ representing the lateral offset.
- $p_2(x|x_1) = p_1(x) - d_1(x|x_1)$, i.e. 2nd round $P_K$ as a function of $x$ given 1st round placed at $x_1$. $d_1(x|x_1)$ reflects the warhead effects of round 1 on $p_1(x_1)$ given its detonation at $x_1$.
- $p_3(x|x_1, x_2) = p_2(x|x_1) - d_2(x|x_1, x_2)$, i.e. 3rd round $P_K$ as a function of $x$ given previous rounds are placed at $x_1$, $x_2$. $d_2(x|x_1, x_2)$ reflects the warhead effects of round 2 on $p_2(x|x_1)$ given $x_1$, $x_2$.
- $p_4(x|x_1, x_2, x_3) = p_3(x|x_1, x_2) - d_3(x|x_1, x_2, x_3)$, i.e. 4th round $P_K$ as a function of $x$ given previous rounds placed at $x_1$, $x_2$, $x_3$. $d_3(x|x_1, x_2, x_3)$ reflects the warhead effects of round 3 on $p_3(x_3|x_1, x_2)$ given $x_1$, $x_2$, $x_3$.
- Placing the 4th round at $x = x_4$, the salvo $P_K$ is then given by: $P(x_1, x_2, x_3, x_4) = p_1(x_1) + p_2(x_2|x_1) + p_3(x_3|x_1, x_2) + p_4(x_4|x_1, x_2, x_3)$.

## 4 IDEALISED MODEL FOR 2-ROUND SALVO

Inspection of warhead effects plots has found that they are often Gaussian in nature and constant in size across placement of the round on its max $P_K$ curve. Also the P(R1)_max plot has an approximate Gaussian shape. These observations suggest approximating these aspects as Gaussian functions calibrated from firing pattern models, and then exploring techniques to optimise aim point placements using these approximations.

An analytical solution to the 2-round salvo problem using Gaussian function approximations is presented here. The 1st round $P_K$ is assumed to be the following Gaussian function:

$$p_1(x) = \kappa_0 e^{-x^2/{\sigma_0}^2}. \quad (1)$$

The warhead effects for this round on $p_1(x)$ given its detonation at $x_1$ is assumed to be

$$d_1(x|x_1) = \kappa_1 \, e^{-(x-x_1)^2/{\sigma_1}^2} \, . \tag{2}$$

The constants $\kappa_0$ and $\kappa_1$ scale the height while the constants $\sigma_0$ and $\sigma_1$ define the breath of the Gaussian functions. The 2nd round $P_K$ as a function of $x$ given placement of the 1st round at $x_1$ is given by

$$p_2(x|x_1) = p_1(x) - d_1(x|x_1) \, . \tag{3}$$

The salvo $P_K$ is obtained by adding together the $P_K$'s for the two rounds placed at positions $x_1, x_2$:

$$P(x_1, x_2) = p_1(x_1) + p_1(x_2) - d_1(x_2|x_1) \, . \tag{4}$$

The positions $x_1, x_2$ that yield the maximum salvo $P_K$ can be obtained through consideration of the critical points of $P(x_1, x_2)$, i.e.

$$\frac{\partial P(x_1,x_2)}{\partial x_1} = 0, \; \frac{\partial P(x_1,x_2)}{\partial x_2} = 0 \, . \tag{5}$$

These equations have the following solution:

$$x_2 = -x_1 \, , \; x_1 = \sqrt{\frac{{\sigma_0}^2{\sigma_1}^2}{4{\sigma_0}^2 - {\sigma_1}^2} \ln\left(\frac{2\kappa_1{\sigma_0}^2}{\kappa_0{\sigma_1}^2}\right)} \, . \tag{6}$$

Results are illustrated using $\kappa_0 = 0.090520$, $\sigma_0 = 74.232$, $\kappa_1 = 0.025868$, $\sigma_1 = 33.305$. The following solution is obtained using the above equations:

$$x_1 = 17.456 \, , \qquad x_2 = -x_1 = -17.456 \, , \qquad P(x_1, x_2) = 0.16268 \, .$$

A spreadsheet model was implemented to verify this solution. The model permits the salvo $P_K$ to be calculated for detonation points specified to the nearest integer. Figure 3 shows the $P_K$ and warhead effects plots from the spreadsheet model for the 2-round example. Plots p1(x) and p2(x|x1) give the $P_K$ curves for the two rounds while p3(x|x1,x2) gives the remaining kill probability after placement of the rounds (this reflects target survivability and would be the $P_{K\_MAX}$ curve for a 3rd round, if considered). The following solution, in agreement with the above analytical results, was obtained for maximising salvo $P_K$:

$$x_1 = 17, \qquad x_2 = -17, \qquad P(x_1, x_2) = 0.16267 \, .$$

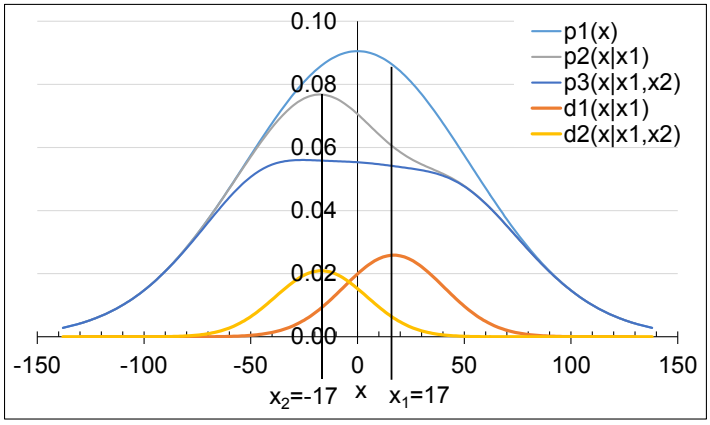


Figure 3: $P_K$ and warhead effects plots from the spreadsheet model for the 2-round example.

## 5 NUMERICAL APPROACH FOR LARGER SALVO SIZES

A salvo consisting of $n$ rounds is considered. The detonation points for each round are given by $x_i,\ i = 1, \dots, n$. $p_1(x)$ is given by equation (1). Warhead effects functions are assumed to be Gaussian and dependent only on the current round, i.e. they are of the form

$$d_i(x|x_i) = \kappa_i\, e^{-(x-x_i)^2/{\sigma_i}^2},\ i = 1, \dots, n\,. \tag{7}$$

The $P_K$ functions for rounds 2 to $n$ are given by

$$p_i(x|x_1, \dots, x_{i-1}) = p_{i-1}(x|x_1, \dots, x_{i-2}) - d_{i-1}(x|x_{i-1}), i = 2, \dots, n\,. \tag{8}$$

The salvo probability of kill for placement of rounds at positions $x_i,\ i = 1, \dots, n$ is given by

$$P(x_1, x_2, \dots, x_n) = \textstyle\sum_{i=1}^{n} p_i(x_i|x_1, \dots, x_{i-1})\,. \tag{9}$$

The probability of kill may be maximized by considering the following extrema of $P$:

$$\frac{\partial P}{\partial x_i} = 0\,, i = 1, \dots, n\,. \tag{10}$$

Putting $f_i = \partial P/\partial x_i$, the system of equations $f_i = 0$ must be solved. Expressing this in vector form with $\mathbf{f}=(f_1, f_2, \dots, f_n)$ and $\mathbf{x}=(x_1, x_2, \dots, x_n)$ gives $\mathbf{f(x)} = 0$. Newton's method is used to find the roots of this system of equations, i.e. find $\mathbf{x}$ such that $\mathbf{f(x)} = 0$. A Taylor`s expansion of $\mathbf{f(x)}$ is given by

$$\mathrm{f(x} + \boldsymbol{\delta}\mathrm{x)} = \mathrm{f(x)} + \mathbf{J}(\mathrm{x})\boldsymbol{\delta}\mathrm{x}\,, \tag{11}$$

where $\boldsymbol{\delta}\mathbf{x} = \mathbf{x^{k+1}} - \mathbf{x^k}$, $\mathbf{x^k}$ is the estimate for $\mathbf{x}$ at the $k$th iteration, and $\mathbf{J}(\mathbf{x})$ is the Jacobian defined by

$$\mathbf{J}(\mathbf{x}) = \frac{\mathrm{d}\mathbf{f}}{\mathrm{d}\mathbf{x}} = \begin{bmatrix} \frac{\partial f_1}{\partial x_1} & \cdots & \frac{\partial f_1}{\partial x_n} \\ \vdots & \ddots & \vdots \\ \frac{\partial f_n}{\partial x_1} & \cdots & \frac{\partial f_n}{\partial x_n} \end{bmatrix}. \tag{12}$$

The solution requires $\mathbf{f(x} + \boldsymbol{\delta}\mathbf{x)} = \mathbf{0}$, and therefore $\mathbf{J}\left(\mathbf{x^k}\right)\boldsymbol{\delta}\mathbf{x} = -\mathbf{f}\left(\mathbf{x^k}\right)$. The definition of $\boldsymbol{\delta}\mathbf{x}$ then permits the estimate $\mathbf{x^{k+1}}$ to be obtained from $\mathbf{x^k}$. The following iterative solution procedure is adopted until a solution of desired accuracy is obtained:

1. Evaluate $\mathbf{f}\left(\mathbf{x^k}\right)$ starting with an initial estimate $\mathbf{x^0}$ for $k = 0$.
2. Compute $\mathbf{J}\left(\mathbf{x^k}\right)$.
3. Solve, using Gaussian elimination, the linear system of equations for $\boldsymbol{\delta}\mathbf{x}$ whose coefficient matrix is $\mathbf{J}\left(\mathbf{x^k}\right)$ and RHS is $\mathbf{f}\left(\mathbf{x^k}\right)$. From this obtain $\mathbf{x^{k+1}}$.
4. Iterate until convergence.

Figure 4 presents results for salvo sizes varying from 2 to 20 in steps of 2. Newton's method finds the roots if the initial guess for $\mathbf{x}$ is reasonably close, otherwise it diverges unless under-relaxation is employed. For $n$ = 2 to 6, the routine converges rapidly, while for $n$ = 16 to 20 it takes 600 to 800 iterations. In all cases aim point offset locations are symmetrical about the $x = 0$ axis, which can be expected as the salvo sizes considered are all even. Salvos with an odd number of rounds will have the first aim point with zero offset, followed by additional aim points having offsets symmetric about the $x = 0$ axis.

As the salvo size increases from $i$ to $i+2$, positioning of rounds 1 to $i$ contracts towards $x = 0$, while positioning of the remaining rounds results in an overall broadening of the firing pattern. The pattern which evolves as salvo size is increased was used to predict round positions for larger salvo sizes, these being used as initial guesses for the Newton's method to improve convergence rates.

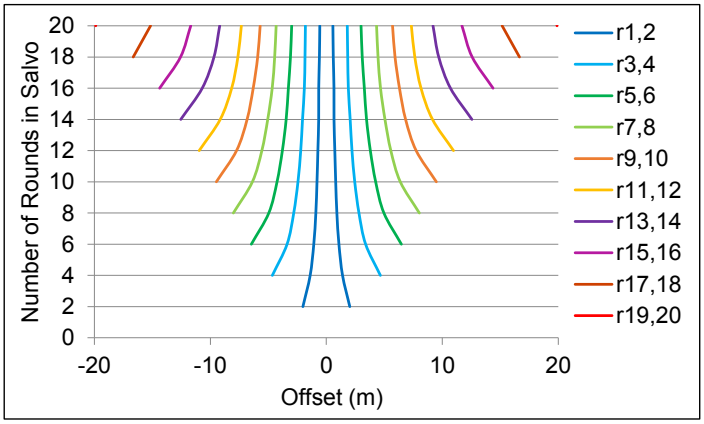


Figure 4: Aim point offset locations for salvos with sizes from 2 to 20 in steps of 2.

## 6 INCORPORATION OF NONLINEAR EFFECTS

The assumptions introduced above, Gaussian function approximations and dependence of warhead effects functions only on the current round, severely restrict application of the method to the actual firing patterns and must be relaxed.

Simple approximations using single Gaussian functions may not be sufficient for representation of the $P_K$ plot for the first round and the warhead effects plots for all rounds – this is clearly evident in Figure 1(b). Improved approximations may be obtained using series of orthogonal polynomials, e.g. Hermite polynomials with Gaussian weighting function (Szegö 1975), or a simple summation of Gaussian functions (Calcaterra and Boldt 2008 for constant variance, Benoudjit et al. 2002 for non-constant variance). The latter approach has been adopted here.

The $P_K$ function for the 1st round can be represented using the following summation of Gaussian functions:

$$p_1(x) = \sum_{i=1}^{N} \kappa_{0,i}\, e^{-\left(x-b_{0,i}\right)^2/\sigma_{0,i}^2}, \tag{13}$$

where $\kappa_{0,i}$, $b_{0,i}$ and $\sigma_{0,i}$, $i = 1, \ldots, N$, are constants chosen to minimise the residue of the approximation.

For the 4-round firing pattern example considered above, Figure 5(a) shows the errors when a single Gaussian function is used to approximate the $P_K$ function for the first round. The Gaussian function was chosen to minimise errors near the peak of the $P_K$ function, but introduces significant errors on the sides. Two additional Gaussian functions are introduced in Figure 5(b) which correct for these errors, with the overall error reduced with a maximum of 0.0018. As shown in Calcaterra and Boldt (2008), further Gaussian functions can be included to reduce the overall error to a desired level. Initial testing has found an additional eight Gaussian functions in approximating p1(x) in Figure 5 will reduce the maximum error to 0.0002.

This approach has also been adopted for approximating the warhead effects functions $d_i$, $i = 1, \ldots, n$. Investigation of these functions from the computational model of Young (2017), however, shows that the parameters $\kappa_i$, $i = 1, \ldots, n-1$, in equation (7) are not constant but are functions of $x_i$. This dependence on $x_i$, $i = 1,2,3$, for the first three rounds is shown in Figure 6(a) for the 4-round example. This graph shows calculation of $\kappa_i$ for warhead effects $P_K$ transformed to the $P_{K\_MAX}$ for the 4th movement zone, each plot

being for the warhead in isolation. The results show the plots to be similar. The 1st round plot has higher $\kappa_1$ (and therefore $P_K$) nearer $x_1 = 0$, this becoming lower as $|x_1|$ increases. This reflects the 1st round movement zone being more condensed near $x = 0$, while movement zones for subsequent rounds have increasing expansion about $x = 0$.

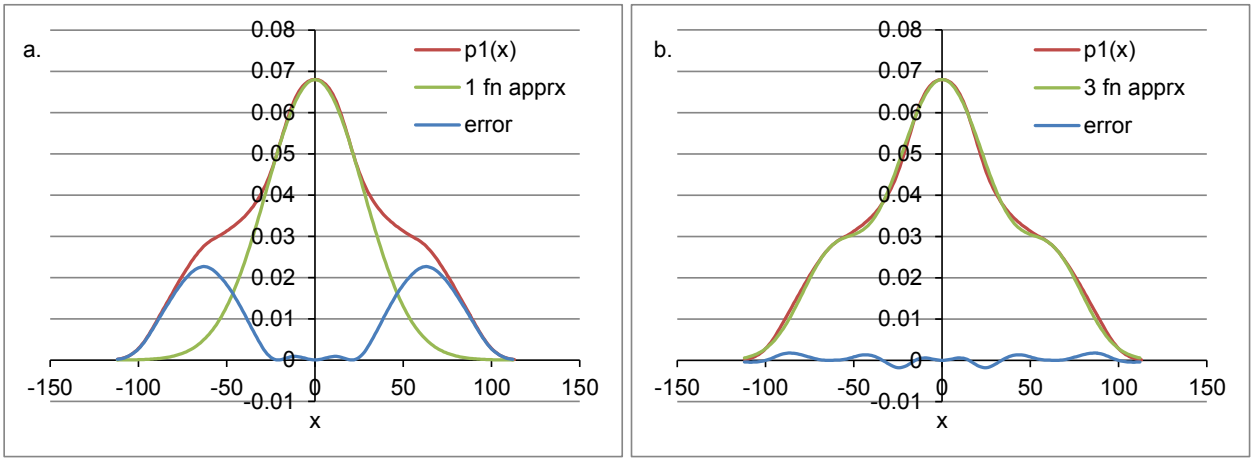


Figure 5: Approximations to 4-round Max $P_K$ curve: (a) Single Gaussian function; (b) Sum of three Gaussian functions.

The results from Figure 6(a) suggest $\kappa_i$ can be represented using the Gaussian function approximation

$$\kappa_i(x_i) = \alpha_i e^{-{x_i}^2/{\beta_i}^2}, \tag{14}$$

with the constants $\alpha_i, \beta_i$ obtained through a calibration from numerical results.

The plots in Figure 6(b) show the translation in the maximum point of the $P_K$ plots from the $P_{K\_MAX}$ curves for the rounds originating movement zone to the movement zone for round 4. This translation accompanies the $P_K$ transformation described above for Figure 2, which results when aligning the $P_{K\_MAX}$ curves for all rounds at the detonation time for the last round. For round 3, the plot is fairly linear indicating the translation has small impact, which can be expected as the translation is done for only one time step, the difference in detonation times from round 4 to round 3. For round 1, the plot becomes nonlinear away from $x_1 = 0$, indicating greater impact of the transformation of the round 1 $P_K$ plot from movement zone 1 to movement zone 4. These "dilation" effects have to be taken into account when mapping backwards from the last movement zone, where the firing pattern optimisation is performed, to earlier movement zones for salvo $P_K$ calculation.

A final aspect that needs to be better represented is the dependence of warhead effects functions $d_i$, $i = 1, \dots, n$, on placement of earlier rounds. Figure 7(a) shows for the 4-round example how $\kappa_2(x_2)$, which relates to round 2 $P_K$, varies with placement of round 2 at $x_2$ for previous placements of round 1 at locations $x_1 = 0, \pm 10, \pm 20$. The graph shows a strong dependence which can be better understood by plotting Figure 7(a) results using abscissa $x_2 - x_1 + c_{2,1}(x_2)$, where $c_{2,1}(x_2)$ is determined empirically to align the curves. This is done in Figure 7(b), the round 2 $P_K$'s being normalized to the maximum values as given in Figure 6(a) for round 2. This process aligns all plots describing dependence of round 2 effects on placement of round 1, although asymmetric effects become prominent as $|x_2|$ increases from 10 to 20. Figure 7(b) results provide a modifier to apply for round 2 $P_K$ calculation given round 1 placement. For round 1 placement directly in line with round 2 (with the $c_{2,1}$ adjustment), the modifier value 0.775 decreases the round 2 $P_K$. The modifier takes on values of 1 when the round 1 placement is sufficiently away from round 2, i.e. round 2 $P_K$ is unaffected by the round 1 placement for $|x_2 - x_1 + c_{2,1}| > 30$.

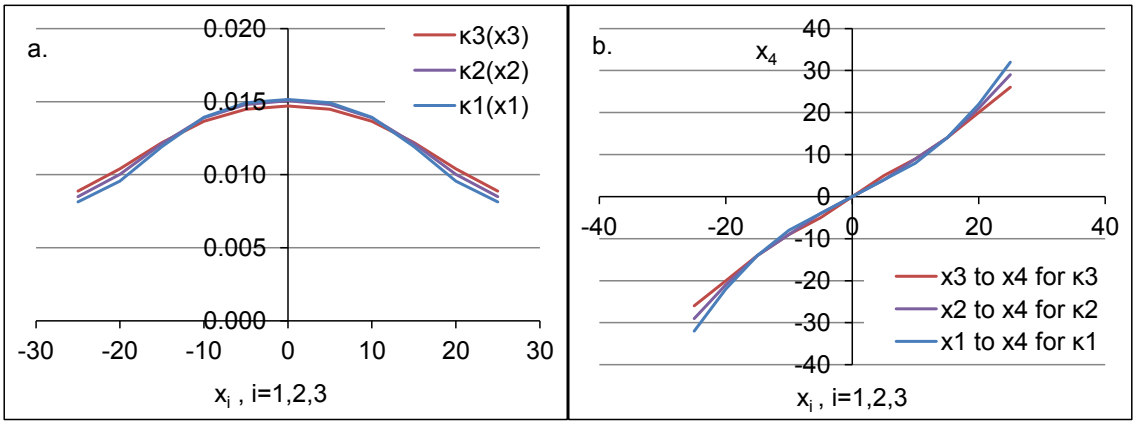


Figure 6: Dependence of warhead effects distribution on lateral offset: (a) Variation in $P_K$; (b) Lateral offset translation to time point 4.

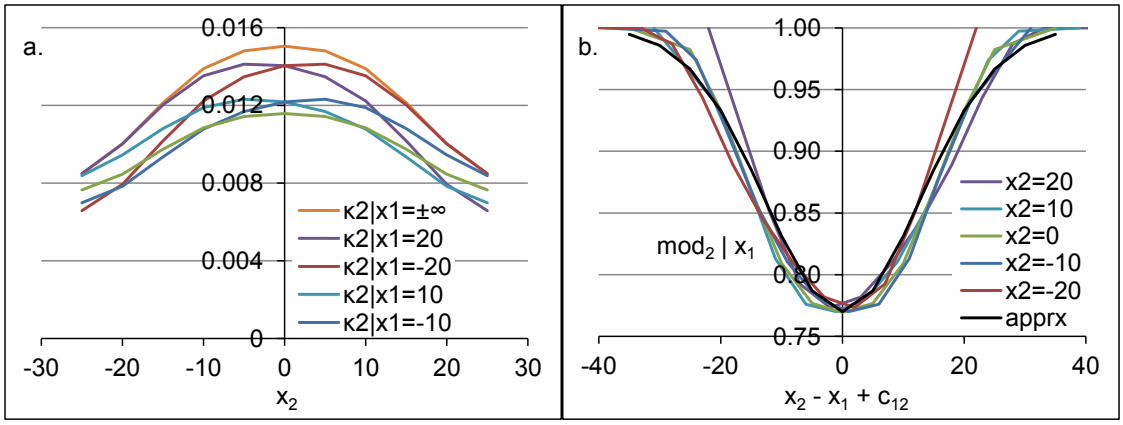


Figure 7: Dependence of round 2 max P(K) distribution on round 1 placement: (a) Variation in round 2 $P_K$; (b) Modifier to round 2 $P_K$.

A modified form of equation (7) which incorporates a Gaussian series approximation and modifiers to account for the above influences on warhead effects is given in (15). The modifiers $\kappa_i(x_i)$ are defined in (14). The modifiers $m_{i,k}$ are defined in (16) and capture the effects depicted in Figure 7(a) applied across all pair-wise combinations of current round-earlier round. The constants $w_{i,k}, \varphi_{i,k}$ are obtained through a calibration from numerical results.

$$d_i(x|x_i,\dots,x_i) = \kappa_i(x_i)\left(\sum_{j=1}^{N}\kappa_{i,j}\, e^{-\left(x-b_{i,j}-x_i\right)^2/\sigma_{i,j}^2}\right)\prod_{k=1}^{i-1}\left(1-\prod_{j=1}^{k} m_{i+1-j,k+1-j}\right). \quad (15)$$

$$m_{i,k} = w_{i,k}e^{-\left(x_i-x_k+c_{i,k}\right)^2/\varphi_{i,k}^2}. \quad (16)$$

These equations in conjunction with equations (8), (9) and (13) constitute a simplified firing pattern model whose data inputs can be calibrated from a more detailed model.

## 7 COMPUTER IMPLEMENTATION

The simplified firing pattern model and optimisation method based on Newton's search with Gaussian elimination for finding local extrema have been implemented in a computer model using Dolphin Smalltalk (2016). The model employs an object-oriented design. Object classes are defined for the basic function

components which make up equations (8), (9) and (13) to (16), including generic function operators for summation and multiplication. An object structure is constructed for the functions in equations (13) and (15). These function objects are used for generating derivative values through the chain rule for an input set of round offsets needed for evaluating equations (10) and (12). An algorithm employing Gaussian elimination is then used to solve (11) from which an updated set of round positions can be obtained. This process is repeated iteratively until convergence to a desired accuracy is obtained.

Testing has shown the optimisation method to be stable with rapid convergence requiring no under-relaxation when the initial positions of the rounds are sufficiently close to a local extrema, e.g. from less than 10 to 250 iterations. Under-relaxation is required for initial positions further away from local extrema. The method has been complemented by a sparse exhaustive search across the full parameter space to enable identification of areas containing local extrema. These areas are then run through the optimiser to find the local extrema, from which a global maximum can then be obtained.

Data inputs for the model include all parameters defining the Gaussian functions and modifiers used for equations (13) and (15). These parameters are obtained through calibration of outputs from a more detailed model, such as that given in Young (1027). The calibration process parallels the analysis outlined above for Figures 5 to 7.

A performance comparison of the optimiser with the detailed model of Young (2017) is given in Table 1 for the 4-round and 6-round firing patterns considered in the next section. The models were executed on an Intel Core i5-5200U processor with 12 GB of memory. The optimiser results are for a calibrated model, the calibration involving a one-time initialisation of the detailed model with post-analysis to produce the required inputs. The initialisation, which involves construction of the $P_{K\_MAX}$ curves for each round, is also required by the detailed model for it to perform single assessments. From Table 1 the optimiser is seen to be 30,000 times faster than the detailed model for a single 4-round pattern assessment, decreasing to 7,000 times for the 6-round pattern. Results in the following section show the optimiser is able to arrive at a firing pattern with local maximum $P_K$ within 250 iterations, the execution time for this being significantly faster than a single assessment of the detailed model.

Table 1: Performance comparison of the optimiser with the detailed model of Young (2017).

| Firing Pattern | Detailed Model | | Optimiser | |
|---|---|---|---|---|
| | Initialisation | Single Assessment | Single Assessment | 250 Iterations |
| 4-Round | 617 s | 22.9 s | 0.00075 s | 0.19 s |
| 6-Round | 1007 s | 34.3 s | 0.0048 s | 1.2 s |

## 8 APPLICATION TO 4-ROUND AND 6-ROUND FIRING PATTERNS

Initial results are presented here for the 4-round firing pattern given in Figure 1 and an expanded 6-round example using the same data inputs. The model and input data from Young (2017) for the 4-round firing pattern were used to provide the calibration inputs for the optimiser. Only a partial calibration was performed at this time, in particular, round 1 interactions on round 2, captured in modifier $m_{2,1}$, were also applied for round 1 interactions on round 3, and round 2 on 3, i.e. $m_{3,2} = m_{3,1} = m_{2,1}$. Additionally, the parameters $c_{i,k}$ in modifiers $m_{i,k}$ have not yet been implemented. Dilation effects are accounted for in mapping round positions from the final movement zone, used by the optimiser, to the movement zones for individual rounds, used by the detailed model.

Preliminary results are summarised in Table 2. Case 1.a shows the results reported in Young (2017), obtained using a heuristic search approach for defining round offsets $x_i$ (first two rounds positioned at peaks of $P_{K\_MAX}$ curves, local search for $x_3$ with $x_4$ computed from its resulting $P_{K\_MAX}$ curve). Case 1.b shows results obtained during further testing of the model from Young (2017), these having the maximum $P_K$ obtained over all cases considered. Cases 1.c and 1.d show results from the optimisation model with round positions mapped back into the individual round movement zones, based on their detonation times, and then evaluated using the model from Young (2017).

Table 2: Comparison of $P_K$ results for round offsets obtained from the firing pattern optimizer.

| Case | Firing Pattern | Method | $x_1, \ldots, x_n$ | $P_K$ | Iterations |
|---|---|---|---|---|---|
| 1.a | 4-Round | Detailed Model: Heuristic | 0, 0, 9.6, -14 | 0.24997 | ~250 |
| 1.b | 4-Round | Detailed Model: Testing | 4, -4, 10, -14 | 0.25022 | ~250 |
| 1.c | 4-Round | Optimiser: Local Max | 1, 2, 14, -14 | 0.24940 | 220 |
| 1.d | 4-Round | Optimiser: Local Max | 8, -15, 5, -6 | 0.24670 | 209 |
| 2.a | 6-Round | Optimiser: Local Max | 0, -1, 15, -15, 50, -54 | 0.30808 | 226 |
| 2.b | 6-Round | Detailed Model: Local Max | 0, 0, 10, -11, 46, -50 | 0.31400 | 25 |

Case 1.c used the initial position from Case 1.a for the optimisation run. The resulting position after execution of the optimiser was (1, 2, 14, -14), which then yielded a $P_K$ of 0.24940 when considered back in the detailed model. This is a slight decrease of 0.23% in $P_K$ and shift in position from the results of Case 1.a. Case 1.c results were also obtained when the initial position from Case 1.b was used, i.e. the two separate initial positions from Cases 1.a and 1.b both converged to the same solution in the optimiser.

Case 1.d results were obtained by the optimiser when the initial value (12.2, -22.5, 7.1, -7.0) was used. This position was obtained from a sparse exhaustive search of the simplified model across the parameter space for round offsets. For this situation the optimiser found a second local extrema with a slightly reduced $P_K$ from that found for Case 1.c.

Initial 6-round results are presented in Case 2.a for the optimiser and Case 2.b for the detailed model. The optimiser used the calibrations obtained for the 4-round example, noting that extrapolation was used to extend the position translations given in Figure 6(b) for the additional two time points and wider breath of the 6-round firing pattern. Case 2.b results were obtained using a limited local search with the detailed model about the Case 2.a position. This found a nearby position with $P_K$ increased by 2%.

The results in Table 2 indicate the optimiser is successful in finding firing patterns with maximum salvo $P_K$'s that approach those obtained from the more detailed model. This is done in significantly faster execution time, given the times per iteration (single assessment) from Table 1. It should be noted that all $P_K$ results in Table 2 were obtained from the detailed model of Young (2017), only the round positions used for Cases 1.c, 1.d and 2.a were obtained from the optimiser. These results indicate a generally flat structure of the salvo $P_K$ surface, with respect to the parameter space defined by round offsets. This flatness results in the optimiser finding different local extrema, based on the initial positions used. Further investigation using the models is required to understand the topology of the salvo $P_K$ surface and dependence on errors, such as those introduced by the Gaussian approximation for $p_1(x)$ in equation (13).

## 9 CONCLUDING REMARKS

A theoretical model based on Gaussian function approximations for warhead effects has been developed for analysis of firing patterns in context of a single engagement assessment. A calibration of the model using results from Young (2017) and its computer implementation have demonstrated the model can be used to rapidly explore a parameter space using optimisation techniques for identification of firing patterns which maximise salvo kill probability. The results indicate the model is able to find "near optimal" solutions in a much faster run time, noting that not all aspects of the model have been calibrated and its accuracy can be improved. Further work has been identified to expand and increase the accuracy of the calibration of the simplified model, and continue testing and cross-model validation for larger salvo sizes, for which the performance difference between the simplified and detailed models will become more pronounced.

The simplified model offers potential to support development of firing patterns by complementing more detailed and robust modelling with high fidelity Monte Carlo simulations, or using methods such as that presented in Young (2017). Outputs from analysis using these techniques can then be used for tactics development and to define firing doctrine for a gun control system, either through lookup tables based on

characteristics defining engagement situations, or using fast running meta-models, such as that presented by the simplified model.

The simplified model also has potential to support firing pattern selection, with associated round expenditure, and engagement assessment within higher level models, such as those presented in Mirshak et al. (2010). The current analysis has focused on assessment of a single engagement, i.e. firing of a single salvo against a single target for a specified range and particular target manoeuvre assumptions. Range and manoeuvre assumptions would vary as the target closes on the defending ship using a weaving path. Young (2017) presents analysis of how firing patterns would vary for different target ranges and manoeuvre assumptions. Each one of these situations would require changes in the calibration inputs to the simplified model. The model complemented by high fidelity simulations could then be used to investigate firing strategies for engagement of multiple threats concurrently attacking one or more defending ships.

A further application of simplified models as presented here and in Mirshak et al. (2010) is to support development of automated battle planning systems for combat simulations, e.g. Harder et al. (2017), or provide assessment algorithms for naval combat management systems, see Benaskeur et al. (2008). For both applications the simplified models offer means to perform rapid engagement assessments for providing inputs into autonomous/semi-autonomous decision making processes.

## REFERENCES


Friedman, N. 2013. *Naval Anti-Aircraft Guns and Gunnery*. Barnsley, U.K: Seaforth Publishing.

Mirshak, R., M. West, and P. Chircop. 2010. "Risk Models for Maritime Security, Area and Port Force Protection". In *Proceedings of the 2010 International Waterside Security Conference*, November 3rd – 5th. Carrara, Italy, 1-8. https://ieeexplore.ieee.org/document/5730263.

Young, P.J. 2017. "Determination of Naval Gun System Firing Patterns to Combat Manoeuvring Surface Targets". In *Proceedings of the 34th International Symposium on Military Operational Research*, July 18th – 21st. London, United Kingdom, 1-21. http://www.ismor.com/ismor2017_papers.shtml.

Szegö, G. 1975. *Orthogonal Polynomials*. 4th ed. New York, US: American Mathematical Society.

Calcaterra, C. and A. Boldt. 2008. "Approximating with Gaussians". arXiv preprint arXiv:0805.3795. https://arxiv.org/pdf/0805.3795.pdf, accessed Mar. 28, 2018.

Benoudjit, N., C. Archambeau, A. Lendasse, J. Lee, and M. Verleysen, M. 2002. "Width Optimization of the Gaussian Kernels in Radial Basis Function Networks". In *Proceedings of the 2002 European Symposium on Artificial Neural Networks*, April 24th – 26th. Bruges, Belgium, 425-432. https://www.elen.ucl.ac.be/esann/proceedings/papers.php?ann=2002.

Dolphin Smalltalk. 2016. Object Arts. http://www.object-arts.com/dolphin7.html, accessed Mar. 28, 2018.

Harder, B., C. Blais, and I. Balogh. 2017. "Conceptual Framework for an Automated Battle Planning System in Combat Simulations". In *Proceedings of the 2017 Winter Simulation Conference*, edited by W. K. V. Chan et al., 4141–4152. Piscataway, New Jersey: IEEE.

Benaskeur, A., E. Bosse, and D. Blodgett. 2008. "Multi-agent Coordination Techniques for Naval Tactical Combat Resources Management". DRDC Valcartier TR 2006-784. Defence Research and Development Canada, Valcartier, Canada.


## AUTHOR BIOGRAPHY


**PETER J. YOUNG** is a Defence Scientist with the Centre for Operational Research and Analysis, Defence Research and Development Canada. He is currently assigned to the Operational Research Team with the Canadian Forces Maritime Warfare Centre supporting the Above Water Battlespace. He holds a Ph.D. in Applied Mathematics from the University of Western Ontario. His research interests include simulation and numerical analysis applied to problems in military operational research. His email address is peter.young2@forces.gc.ca.